Using texture components in crystal plasticity finite element simulations

Dierk Raabe*, Franz Roters

Max-Planck-Institut für Eisenforschung, Max-Planck-Straße 1, 40237 Düsseldorf, Germany

Abstract

We discuss methods to map crystallographic textures in crystal plasticity finite element simulations. Fourier-type series expansion methods which use spherical harmonic library functions as well as the direct pole figure inversion methods are not well suited to reproduce texture information in a sufficiently localized spherical form onto finite element grids. Mathematically compact Gauss-shaped spherical texture components represent a better approach for including textures in finite element models since they represent an excellent compromise between discreteness (spherical localization), compactness (simple functions), mathematical precision (very good approximation also of complex orientation distribution functions already with small sets of texture components), scalability (the number of used texture components can be systematically varied according to the desired exactness of the texture fit), conceptual simplicity (simple mathematical handling), and physical significance (texture components can be directly linked to characteristic metallurgical mechanisms). The use of texture component functions has also advantages over the use of large sets of discrete single orientations with equal scatter and height since they are more compact, practical, and provide better physical insight into microstructural mechanisms and composition sensitive effects. The article presents a new approach for the mathematical reproduction of such crystallographic texture components in crystal plasticity finite element simulations. It explains in some detail why they are particularly suited for this purpose and how they can be used to map and recover textures in/from plasticity simulations.
© 2003 Elsevier Ltd. All rights reserved.

Keywords: Texture; Crystal plasticity; Anisotropy; Orientation distribution function; Simulation; Polycrystal; Microstructure; Constitutive behavior

* Corresponding author. Tel.: +49-211-6792-340; fax: +49-211-6792-333.
  E-mail address: raabe@mpie.de (D. Raabe).

1. Introduction

Metals mostly occur in polycrystalline form where each grain has a different crystallographic orientation, shape, and volume fraction. The distribution of the grain orientations is referred to as crystallographic texture (Wassermann and Grewen, 1969; Bunge, 1982). The discrete nature of crystallographic slip along certain lattice directions on preferred crystallographic planes entails an anisotropic plastic response of such samples under mechanical loads (Hosford, 1996; Kocks et al., 1997; Zhou et al., 1998; Bhattacharyya et al., 2001; Nakamachi et al., 2002). While the elastic–plastic deformation of single crystals and bicrystals can nowadays be well predicted, plasticity of polycrystalline matter is less well understood. This is essentially due to the intricate interaction of the grains during co-deformation (Beaudoin et al., 1995, 1996; Raabe, 1995a,b; Van Houtte et al., 2002). This interaction leads to strong in-grain and grain-to-grain heterogeneity in terms of strain, stress, and crystal orientation (Fig. 1) (Raabe et al., 2001a,b, 2002a,b,c).

One major aim of polycrystal research consequently lies in identifying adequate measures for mapping initial crystallographic anisotropy into mathematical methods for predicting large strain plastic deformation of polycrystalline matter. The second even more demanding goal is the prediction of the *evolution* of crystalline anisotropy during plastic deformation. This is necessary since the crystals individually rotate during deformation owing to the nonsymmetry of the displacement gradients created by crystal slip. The complex microstructural processes involved during these reorientation processes of the individual grain portions in polycrystalline matter
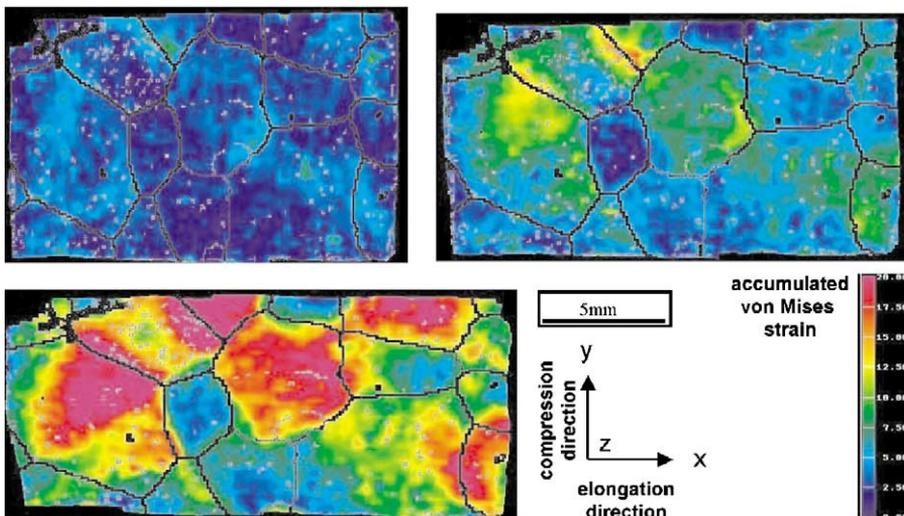

Fig. 1. Experimentally observed distribution of the accumulated plastic von Mises strain in a coarse grained aluminium specimen after 3, 8, and 15% sample thickness reduction (given in terms of $\Delta d/d_0 \times 100\%$, where d_0 is the sample extension along compression direction prior to deformation). The strains were determined using optical photogrametry (Raabe et al., 2001a,b). The grain boundaries indicated by black lines were taken from microtexture measurements conducted in a scanning electron microscope.

cannot be captured in terms of simple empirical constitutive laws but require the use of physically-based concepts. In this context the crystal plasticity finite element constitutive methods have increasingly gained momentum (Mathur and Dawson, 1989; Kalidindi et al., 1992; Sarma and Dawson, 1996; Mika and Dawson, 1999; Bhattacharyya et al., 2001; Kalidindi, 2001; Kok et al., 2002). In these approaches one typically assumes the stress response at each macroscopic continuum material point to be potentially given by one crystal or by a volume-averaged response of a set of grains comprising the respective material point. The latter method naturally involves local homogenization. Compared to isotropic J2 approaches the crystal plasticity finite element method reduces the degrees of freedom for the displacement field at each integration point to the crystallographic slip dyades transformed according to the local grain orientation. Representing and updating the crystallographic orientation at each Gauss point renders crystallographically discrete plasticity simulations powerful tools for investigating anisotropy and the evolution of deformation textures.

The current study addresses the question how crystallographic textures can be merged with crystal plasticity finite element constitutive descriptions in a more rigorous, scalable, and efficient way (Zhao et al., 2001; Raabe et al., 2001a,b, 2002a,b,c). A special challenge in this context lies in the reduction of redundant texture information to a level where sufficient details can be recovered without loosing physical significance. This point requires some explanation. Modern experimental and theoretical acquisition methods for crystallographic textures typically facilitate and in part necessarily entail the accumulation of data sets consisting of huge numbers of single crystallographic orientations. An example known from experimental texture research is the use of crystal orientation mapping methods (microtexture, discrete texture with lateral resolution). This is a technique for analyzing the two dimensional topology of crystallographic texture and grain boundaries in crystalline material. Local lattice orientations are measured on a regular grid by automated acquisition and processing of electron backscatter diffraction patterns (Kikuchi patterns) in a scanning electron microscope. The microstructure can subsequently be reconstructed by coloring similar orientations on the measured grid with similar colors which are chosen in accord with the position of that orientation in Euler space. In addition to that the quality of the Kikuchi patterns can be determined for each lattice point as a measure for the local perfection of the crystal lattice. Current orientation mapping methods in the scanning electron microscope typically work with lateral resolutions between 15 nm and 15 μm and allow the skilled user to measure up to 45 single orientations per second when using electron beam control mode. However, the use of such huge discrete single orientation arrays as data input for subsequent crystal plasticity finite element simulations is often neither practical nor scientifically rewarding since it provides more texture information than is usually necessary for predicting plastic anisotropy of formed parts and the evolution of texture. Similar arguments apply when feeding textures into crystal plasticity finite element simulations which were obtained from two-dimensional centro-symmetric pole figures measured by X-ray or neutron diffraction and inverted by employment of series expansion techniques or direct inversion methods (macrotexture, statistical texture without lateral resolution).

This rather complex problem of representing large microtexture or macrotexture sets in plasticity simulations can be split into two quite separate tasks. The first one is the formulation of a basic solution method which uses crystallographic orientation as a state variable. This is typically achieved by formulating an orientation dependent constitutive law which maps the requested physical anisotropy at the single crystal scale and by embedding this formulation into a finite element code (Asaro and Needleman, 1985; Mathur and Dawson, 1989). The numerical implementation then tackles the interaction of the differently oriented volume portions and thereby predicts the integral response of the sample under loads. Any such formulation requires a *discrete* representation of the orientation distribution function or a portion of it at each integration point. Therefore, the second task consists in feeding one *single* rotation matrix (crystal orientation) directly on each Gauss point of the finite element mesh. This amounts to mapping or respectively decomposing orientation distributions in such a way that they can be subsequently mapped on a mesh in a discrete manner thereby matching the initial overall distribution.

One method to map large texture data sets onto a discrete mesh could be to simply assign each prescribed or measured discrete orientation matrix to an individual grid point. This is indeed the classical approach which is currently used by many crystal plasticity finite element modelers (Mathur and Dawson, 1989; Kalidindi et al., 1992; Beaudoin et al., 1995; Sarma and Dawson, 1996; Raabe and Becker, 2000; Bhattacharyya et al., 2001; Kalidindi, 2001; Raabe et al., 2001a,b). However, such an orientation-by-orientation (or grain-by-grain) approach is not practicable when conducting forming simulations of larger parts typically containing more than 10^{10} separate crystals. The second idea, therefore, is to formulate a *scalable* method for including textures in crystal plasticity finite element simulations. Scalability means in this context to feed large as well as small texture data sets into finite element models, but with an exact quantification of the crystallographic error arising from such data reduction.

Before discussing the advantages and disadvantages of the various functions available for the reproduction of textures it must be noted that crystal plasticity finite element approaches require a *discrete* representation of the orientation distribution function or a portion of it at each integration point. Mapping a discrete part of a global texture to a Gauss point or to a set of Gauss points requires a method which is physically meaningful (avoiding over-simplification) and which at the same time reduces the texture information content to a level which is necessary to treat complex forming situations at reasonable computation costs (avoiding over-modeling). Such a form is offered in particular by the texture component method (Lücke et al., 1981; Matthies, 1982; Lücke et al., 1986; Helming and Eschner, 1990; Helming et al., 1994; Eschner, 1994; Eschner and Fundenberger, 1997). It approximates the orientation distribution function by a superposition of sets of simple standard functions with individual spherical coordinates, orientation density, and scatter in orientation space. Such a representation of a preferred orientation is referred to as a texture component. In contrast to the use of global symmetric Wigner functions for instance in the Fourier-type series expansion methods (Bunge, 1982, 1987), the texture component method is based on using localized spherical normalized standard functions.

The new concept we therefore suggest for representing textures efficiently in plasticity simulations is based on mapping small sets of mathematically compact spherical Gaussian texture components on the integration points of a crystal plasticity finite element model (Zhao et al., 2001; Raabe et al., 2001a,b). This is done in two steps: first, by extracting the texture components and the random background from experimental starting textures according to the method of Helming et al. (1994). Second, by decomposing these functions into sets of discrete orientations which altogether exactly represent the original Gauss shape of each component (in orientation space) so that they can be mapped as lateral distributions onto a discrete lattice. The initial spherical distribution is thereby transformed into a spherical *and* lateral distribution.

During the subsequent crystal plasticity finite element simulation the texture component method loses its significance since each individual orientation originally pertaining to one of the texture components can undergo *individual* re-orientation as in any of the above quoted crystal plasticity methods. In order to avoid confusion one should, therefore, underline that the texture component method is used to *feed* textures into finite element simulations on a strict physical and quantitative basis. The components as such, however, are not further tracked as functions during the simulation. On the other hand the mapped orientation points which were extracted from the components must not be confused with individual grains, but they are points of a distribution function.

The texture component approach ensures that the mapping of textures can be linked to materials concepts since texture components can be directly interpreted in terms of characteristic metallurgical mechanisms. Furthermore it makes sure that redundant texture information which is less relevant, for instance to predict plastic anisotropy, can be reduced in the input data set. The following chapters explain the method in more detail and give examples.

2. Texture functions

2.1. Reproduction of the orientation distribution function

The orientation distribution of the grains and subgrains assembling a polycrystalline aggregate, $f(g)$, can be reproduced from two-dimensional centro-symmetric projections which are referred to as pole figures or from sets of single orientations (Bunge, 1982, 1987; Matthies et al., 1988; Matthies, 1991). In either case different mathematical techniques can be used. In the first case the orientation distribution is commonly described in terms of the direct inversion of the pole figures or in terms of Fourier-based series expansion methods which use spherical harmonics as library functions. In the second case one commonly reproduces the orientation distribution by use of large sets of discrete single grain orientations with identical scatter and amplitude or by use of the texture component method where each preferred orientation has *individual* scatter and amplitude. Overviews were given by Bunge (1982, 1987), Matthies et al. (1987–1990), Wenk et al. (1988), and Kocks et al. (1997).

2.2. Direct pole figure inversion

The direct inversion methods approximate textures in terms of the integration of the fundamental equation of texture analysis using a set of experimental pole figures (Bunge, 1987; Wenk et al., 1988; Raabe and Lücke, 1993, 1994). Since they directly use the discrete form of the fundamental equation for pole figure inversion they work in real space and not in Fourier space. This means that these approaches make use of the fact, that the discrete hemisphere of the pole figure corresponds to families of projection tubes in the $f(g)$ space, i.e. the non-negativity condition for the orientation distribution function is automatically taken into account (Wenk et al., 1988; Bunge, 1987). The solution is achieved by iteration. The direct methods are—like all texture reproduction methods which use starting data of higher symmetry (i.e. 2D projections obtained under the limitation of Friedel's law[1]) than the orientation distribution function—affected by the inversion symmetry of the pole figure data entailing positive or negative texture portions in the spherical 3D distribution without physical significance (texture ghosts). In the discrete form, cells in the pole figures and in the $f(g)$ space are directly related by linear equations. The density in each pole figure cell is the sum of the corresponding cell densities in the $f(g)$ space. Since different $f(g)$ sums lead to the same pole density, the set of linear equations is underdetermined which leads to so called ghost errors in the orientation distribution function. The second disadvantage of the direct inversion methods is that they do not provide Fourier coefficients. Although this shortcoming is inevitably connected with all direct approaches it can be avoided by subsequently fitting an orientation distribution function derived by direct inversion using a series expansion method. Fourier coefficients of texture functions are generally desirable because they facilitate the calculation of anisotropic behavior such as directional elastic, magnetic, or electrical properties of polycrystalline aggregates from texture data. Although directional physical properties are of course not necessarily connected to Fourier coefficients, their employment permits high speed calculations of data of textured samples particularly in cases where homogenization theory is used to couple texture and properties.

2.3. Fourier-type series expansion methods

In the various Fourier-type series expansion methods the orientation distribution function is approximated by computing the coefficients $C_l^{\mu v}$ of its orthogonal expansion from the expansion coefficients $F_l^v(h_i)$ of experimentally detected pole figures (Bunge, 1982, 1987). Since the centro-symmetric pole figures are expanded with a series of even order spherical harmonics, only the even order coefficients $C_l^{\mu v}$ of $f(g)$ are generated (see footnote on Friedel's law), rendering the so determined function an approximate orientation distribution function containing only the even part of $f(g)$ which is referred to as $\tilde{f}(g)$.

---

[1] Friedel's law states that pole figure projections can not differentiate between the northern and the southern hemisphere in the common case that non-polarized beams are used for the experiment.

The complete function, $f(g)$, is named true orientation distribution function. The real orientation distribution is hence given by the equation $f(g) = \tilde{f}(g) + \tilde{\tilde{f}}(g)$, where $\tilde{\tilde{f}}(g)$ represents any function which can be added to $\tilde{f}(g)$ without changing corresponding projections, i.e. pole figures (Matthies et al., 1988; Matthies, 1991). The even function $\tilde{f}(g)$ usually causes texture dependent errors (ghost peaks). These adulterations can either be positive or negative. For reducing such ghost intensities in the orientation distribution function advanced series expansion methods use the non-negativity condition which led to the development of an iterative series-expansion method (Bunge, 1987; Dahms et al., 1994; Raabe, 1995).

2.4. Texture component methods

A third important method for reproducing orientation distributions are Gauss- or Lorentz-based model functions with individual height and individual full width at half maximum as a measure for the strength and scatter of a crystallographic texture component (Lücke et al., 1981, 1986; Matthies, 1982; Helming and Eschner, 1990; Helming et al., 1994; Helming, 1996; Eschner and Fundenberger, 1997). This approach is referred to as texture component method. It goes back to the early texture studies where experimental and predicted pole figures were mostly interpreted in terms of the evolution and physical significance of discrete texture components (Wassermann and Grewen, 1969). Classical terms introduced in these early studies on crystallographic orientation distributions were for instance the "Copper texture component", the "Brass texture component", and the "Taylor texture component". The use of preferred orientations prevailed in texture research until the late sixties of the last century, i.e. statements about texture evolution were made practically exclusively on the basis of pole figures and estimated preferred components (ideal positions, texture components). Modern approaches which describe texture components in orientation space (Lücke et al., 1981, 1986; Matthies 1982; Helming and Eschner, 1990; Helming et al., 1994; Helming, 1996; Eschner and Fundenberger, 1997) approximate the orientation distribution function by a superposition of sets of Gauss- or Lorentz-shaped model functions with individual height and individual full width at half maximum as a measure for the strength and scatter of a crystallographic texture component in orientation space. While the early texture components concepts use *central* functions which have an *isotropic* scatter in orientation space, the approach of Eschner and Fundenberger (1997) even allows one to employ asymmetric texture functions which use different scatter in different orientation directions. In contrast to the use of global symmetric Wigner functions for instance in the Fourier-type series expansion methods, the texture component method is based on using localized spherical normalized standard functions.

The described properties qualify the texture component approach as a method for extracting texture information in a compact fashion from experiment or theory and subsequently decomposing and feeding it into finite-element based anisotropy simulations which involve very large numbers of grains.

The following section will give a concise mathematical review of the texture component method and explain how texture components can be mapped on a finite element

grid in cases where the underlying constitutive model has been formulated in an orientation dependent fashion.

3. Basic formulation of the texture component method for the crystal plasticity finite element approach

Following the pioneering work of Lücke et al. (1981, 1986) as well as the formulations suggested by Helming and Eschner (Eschner, 1994; Helming and Eschner, 1990; Helming et al., 1994; Helming, 1996) the mathematical reproduction of the orientation distribution function by texture component functions which are locally restricted in orientation space can be expressed by the superposition

$$f(g) = F + \sum_{c=1}^{C} I^c f^c(g) = \sum_{c=0}^{C} I^c f^c(g) \quad \text{where} \quad I^0 = F, f^0(g) = 1 \tag{1}$$

where g is the orientation, $f(g)$ is the orientation distribution function and F is the volume portion of all randomly oriented crystals (random texture component). F may be understood as the intensity of the only *global* component used in the approximation, equivalent to $f^c(g) = 1$ for each orientation point in Euler space, $g \in G$. The intensity I^c describes the volume fraction of all crystallites belonging to the component c. Fig. 2 shows a schematical sketch of a spherical texture component c which is described in terms of a maximum orientation density at a preferred orientation g^c and scatter width b^c (Helming, 1996). The orientation density of the component is described by a central function, i.e. its value decreases isotropically with increasing orientation distance $\tilde{\omega}^c = \tilde{\omega}(g^c, g)$ from the maximum. This means
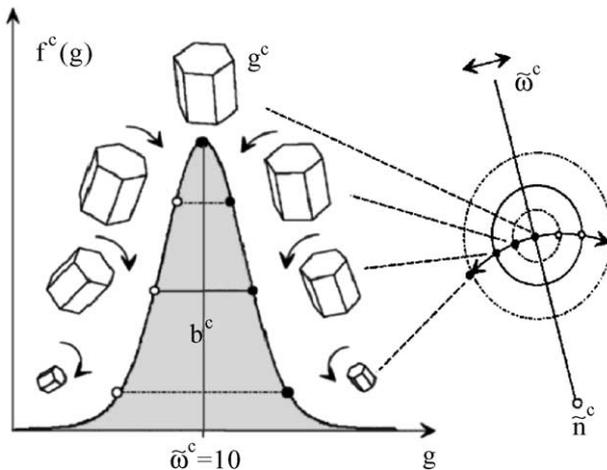

Fig. 2. Schematical presentation of a spherical texture component c with a preferred orientation g^c and scatter width b^c. $f^c(g)$ only depends on $\tilde{\omega}^c = \tilde{\omega}(g^c, g)$, i.e. it is independent on the rotation axis $\tilde{n}^c$ (Helming and Eschner, 1990; Helming et al., 1994; Helming, 1996).

that $f^c(g)$ only depends on $\tilde{\omega}^c = \tilde{\omega}(g^c, g)$ and is independent on the rotation axis $\tilde{n}^c$. A more comprehensive definition of texture functions was given by Eschner (1994) who suggested texture components with an anisotropic spherical scatter. The use of such more complex texture component functions is, however, less well suited for the texture component crystal plasticity finite element method due to the increase in the number of required parameters.

The orientation distribution function is defined by

$$f(g)\mathrm{d}g = 8\pi^2 \frac{\mathrm{d}V_g}{V} \quad \text{which implies} \quad f(g) \geqslant 0 \tag{2}$$

where V is the sample volume and $\mathrm{d}V_g$ the volume of all crystals with an orientation g within the orientation portion $\mathrm{d}g = \sin(\varphi)\,\mathrm{d}\varphi\,\mathrm{d}\varphi_1\,\mathrm{d}\varphi_2$. Normalization requires

$$\oint f^c(g)\mathrm{d}g = 1 \quad \text{which implies} \quad \sum_{c=0}^{C} I^c = 1 \tag{3}$$

As a rule texture components require positivity, i.e.

$$f^c(g) \geqslant 0 \quad \text{for all} \quad g \in \quad \text{and} \quad I^c > 0 \tag{4}$$

where G is the orientation space. Eq. (4) can also be derived by using Eq. (2) and the assumption that the texture components do not overlap in orientation space and that an orientation distribution function can be described by one single texture component.

Distribution functions which have a maximum at a preferred orientation g^c and decrease with increasing orientation distance $\tilde{\omega}^c = \tilde{\omega}(g^c, g)$ are referred to as central functions. Such functions, including corresponding pole figures, can be generally represented in the form of series expansions of χ functions or respectively Legendre polynomials. More practical approximations of texture components have been introduced on the basis of spherical Gauss- and Lorentz-functions. The examples presented later in this work make use of Gauss-shaped model functions for the decomposition of the orientation distribution function which are described by

$$f^c(g) = N^c \exp(S^c \cos\tilde{\omega}) \tag{5}$$

where

$$S^c = \frac{\ln 2}{1 - \cos(b^c/2)} \quad \text{and} \quad N^c = \frac{1}{I_0(S^c) - I_1(S^c)} \tag{6}$$

The according pole figure projections $P_h^M(g^c, b^c, y)$ can be calculated in closed analytical form

$$P_h^M(g^c, b^c, y) = N^c \exp(S^c \sin(\upsilon^c/2))\, I_0(S^c \cos(\upsilon^c/2)) \tag{7}$$

where υ^c describes the geometry of the component in the respective pole figure projection and $I_l(x)$ are generalized Bessel functions. The value b^c is the halfwidth and can be interpreted as the mean diameter of a spherical component in orientation space (Helming et al., 1994; Helming, 1996).

The components describing $f(g)$ can be determined by the best fit of the experimental pole figure input data $\tilde{P}_{h_i}^M(y_r)/N_{h_i}$ with the recalculated pole figures $\sum_c I^c \tilde{P}_h^M(g^c, b^c, y_r)$. The index r marks the measured sample directions y_r. The component parameters I^c, g^c and b^c and the normalization N_{h_i} of the pole figures are obtained by solving the least squares problem

$$\sum_{i,r} w_{ir} \left[\tilde{P}_{h_i}(y_r)/N_{h_i} - \sum_c I^c \tilde{P}_{h_i}^M(g^c, b^c, y_r) \right]^2 \Rightarrow \text{Min.} \tag{8}$$

where w_{ir} are weight factors. Usually the parameters g^c and b^c must be calculated by a non-linear algorithm. First estimates are required, which may be obtained manually from the graphical representation of the difference pole figures which are calculated according to

$$\Delta_{h_i}(y_r) = \tilde{P}_{h_i}(y_r) - \sum_c I^c \tilde{P}_{h_i}^M(g^c, b^c, y_r) \tag{9}$$

Depending on experience in interpreting crystallographic textures the user can specify the position, height, and scatter of the texture components within certain bounds before the minimization. This makes particularly sense, when the number of texture components initially prescribed to match an experimental texture is small or when a certain scatter width of the components should not be exceeded. Further details on the method are given in the works of Lücke et al. (1981, 1986) and Helming and Eschner (Eschner, 1994; Helming and Eschner, 1990; Helming et al., 1994; Helming, 1996). The texture component version used for this study is the one described by Helming (1996).

4. Important texture components

The texture component method provides a small set of compact functions which are characterized by simple parameters of physical significance (Euler angles, scatter, volume fraction). Usually, only a few texture components are required for representing textures in a precise mathematical form and to account for the plastic anisotropy. The inherent data reduction drastically enhances the computational efficiency of the subsequent finite element simulation.

The textures of polycrystalline matter can be reproduced by using small sets of discrete texture components together with a random background component. The most important of these components in face centered cubic metals are the Cube-component ($\{001\}<100>$, $\varphi_1 = 0°$, $\varphi = 0°$, $\varphi_2 = 0°$), the Goss-component ($\{011\}<100>$, $\varphi_1 = 0°$, $\varphi = 45°$, $\varphi_2 = 0°$), the Brass-component ($\{0\underline{1}1\}<211>$, $\varphi_1 = 35°$, $\varphi = 45°$, $\varphi_2 = 0°$), the Copper-component ($\{\underline{2}11\}<111>$, $\varphi_1 = 90°$, $\varphi = 35°$, $\varphi_2 = 45°$), and the S-component ($\sim\{12\underline{3}\}<634>$, $\varphi_1 = 60°$, $\varphi = 32°$, $\varphi_2 = 65°$).

In body centered cubic metals the most important texture components are the Rotated Cube component $\{001\}<110>$ ($\varphi_1 = 0°$, $\varphi = 0°$, $\varphi_2 = 45°$), the Inverse Brass-component $\{1\underline{1}2\}<110>$ ($\varphi_1 = 0°$, $\varphi = 35°$, $\varphi_2 = 45°$), the $\{1\underline{1}1\}<110>$ component

($\varphi_1 = 0°$, $\varphi = 54.7°$, $\varphi_2 = 45°$), the $\{111\} <11\underline{2}>$ component ($\varphi_1 = 30°$, $\varphi = 54.7°$, $\varphi_2 = 45°$), and the Goss-component ($\{011\} <100>$, $\varphi_1 = 0°$, $\varphi = 45°$, $\varphi_2 = 0°$).

5. The crystal plasticity constitutive model

In our present approach we use the large-strain constitutive crystal plasticity model suggested by Kalidindi et al. (1992) and Bhattacharyya et al. (2001). In this formulation one assumes the stress response at each macroscopic continuum material point to be potentially given by one crystal or by a volume-averaged response of a set of grains comprising the respective material point. The latter assumption can be referred to as a local Taylor-type or local strain-rate homogenization assumption. In case of a multi-grain description the volume averaged stress amounts to

$$\langle \mathbf{T} \rangle = \sum_{k=1}^{N} (w_k \mathbf{T}_k) \tag{10}$$

where N is the total number of individual orientations mapped onto an integration point using the Taylor assumption, w_k the volume fraction of each single orientation extracted from a texture component as described above, $\mathbf{T}_k$ the Cauchy stress produced by the kth individual orientation, and $\langle \mathbf{T} \rangle$ the volume average stress produced by all orientation mapped at the integration point. The constitutive equation for the stress in each grain is then expressed in terms of

$$\mathbf{T}^* = \mathbf{CE}^* \tag{11}$$

where $\mathbf{C}$ is the fourth order elastic tensor and $\mathbf{E}^*$ an elastic strain measure obtained by polar decomposition,

$$\mathbf{E}^* = \frac{1}{2} \left(\mathbf{F}^{*^T} \mathbf{F} - 1 \right) \tag{12}$$

which leads to a stress measure which is the elastic work conjugate to the strain measure $\mathbf{E}^*$,

$$\mathbf{T}^* = \mathbf{F}^{*^{-1}} (\det(\mathbf{F}^*)\mathbf{T})(\mathbf{F}^*)^{-T} \tag{13}$$

where $\mathbf{T}$ is the symmetric Cauchy stress tensor in the grain, and $\mathbf{F}^*$ is a local elastic deformation gradient defined in terms of the local *total* deformation gradient $\mathbf{F}$ and the local *plastic* deformation gradient $\mathbf{F}^p$. The relation between the elastic and the plastic portion of $\mathbf{F}$ amounts to

$$\mathbf{F}^* = \mathbf{F}(\mathbf{F}^p)^{-1}, \ \det(\mathbf{F}^*) > 0, \det(\mathbf{F}^p) = 1 \tag{14}$$

The plastic deformation gradient is given by the flow rule

$$\dot{\mathbf{F}}^p = \mathbf{L}^p \mathbf{F}^p \tag{15}$$

with its crystalline portion

$$\mathbf{L}^{\mathrm{p}} = \sum_{k=1}^{N} \dot{\gamma}_k \mathbf{m}_k, \ \ \mathbf{m}_k = \hat{\mathbf{b}}_k \otimes \hat{\mathbf{n}}_k \tag{16}$$

where $\mathbf{m}_k$ are the kth dyadic slip products of unit vectors $\hat{\mathbf{b}}_k$ in the slip direction and $\hat{\mathbf{n}}_k$ normal to the slip plane, and $\dot{\gamma}_k$ the shear rates on these systems. The specific constitutive functions for the plastic shearing rates $\dot{\gamma}_k$ on the slip systems are taken as

$$\dot{\gamma}_k = \dot{\gamma}_o \left| \frac{\tau_k}{\tau_{k,\mathrm{crit}}} \right|^{1/m} \mathrm{sgn}(\tau_k) \tag{17}$$

where τ_k is the resolved shear stress for the slip system k, and $\tau_{k,\mathrm{crit}}$ is the actual critical shear stress on the kth slip system. $\dot{\gamma}_o$ and m are material parameters representing shearing rate and the rate sensitivity of slip. The calculation of $\tau_{k,\mathrm{crit}}$ has been achieved by accounting for latent hardening through the use of an appropriate hardening matrix,

$$\dot{\tau}_{k,\mathrm{crit}} = \sum_i h^{ki} |\dot{\gamma}^i|, \ \ h^{ki} = q^{ki} h^{(i)} \tag{18}$$

where h^{ki} is the rate of strain hardening on kth slip system due to a shearing on ith slip system, q^{ki} is the hardening matrix describing the latent hardening behavior of a crystallite, and $h^{(i)}$ is the hardening rate of the single slip system i. In the present study, 12 slip systems with crystallographic $<110>$ slip directions and $\{111\}$ slip planes are taken into account for room temperature simulations of plastic deformation of aluminium. The matrix h^{ki} can be taken as

$$h^{ki} = \begin{bmatrix} A & qA & qA & qA \\ qA & A & qA & qA \\ qA & qA & A & qA \\ qA & qA & qA & A \end{bmatrix} \tag{19}$$

where q is the ratio of the latent hardening rate to the self-hardening rate, and A is a 3×3 matrix populated by ones. Using this constitutive description renders the finite element method an elegant tool for detailed simulation studies of texture evolution and strain distribution under realistic boundary conditions. Each integration point can represent one orientation or map a larger set of crystals as outlined above. The actual finite element calculations were carried out using the finite element software packages ABAQUS and MARC in conjunction with their respective user defined material subroutines (Zhao et al., 2001; Raabe et al., 2001a,b).

6. Mapping texture components in the crystal plasticity finite element constitutive model

One important challenge of polycrystal plasticity simulations lies in identifying an efficient way of mapping *statistical* and *representative* crystallographic orientation

distributions on the integration points of a grid of a crystal plasticity finite element model. This applies in particular when aiming at the simulation of larger parts typically containing more than 10^{10} separate crystals. The new concept we suggest for this task is based on mapping small sets of mathematically compact spherical Gaussian texture components on the integration points of a crystal plasticity finite element model.

Fig. 3 shows the principle of the new approach (Zhao et al., 2001; Raabe et al., 2001a,b). After recovering texture components from experimental or theoretical data according to the method of Helming (Helming et al., 1994; Helming, 1996) as outlined in Section 3 they must be mapped onto the integration points of a finite element mesh. This is conducted in two steps. First, the discrete preferred orientation g^c (center orientation, mean orientation) is extracted from each of the texture components and assigned in terms of its respective Euler triple (φ_1, φ, φ_2), i.e. in the form of a *single* rotation matrix, onto *each* integration point (Fig. 4a). In the second step, the mapped single center orientations of the texture components are rotated in such a fashion that the resulting overall distribution of *all* rotated orientations reproduces exactly the texture function which was originally prescribed in the form of a compact texture component (Fig. 4b). In other words the orientation scatter individually described by each texture component function is mapped onto the finite element by systematically modifying the orientations at each point in a way which exactly imitates the scatter prescribed by the texture component (Fig. 5). This means that the scatter which was originally only given in orientation space is now represented by a distribution both, in real space and in orientation space, i.e. the initial spherical distribution is transformed into a spherical *and* lateral distribution. It is important in this context, that the use of the Taylor assumption locally allows one to map more than one preferred crystallographic orientation on each integration point and to assign to them different volume fraction (Fig. 6). This means that the procedure of mapping and rotating single orientations in accord with the initial texture component scatter width is individually conducted for *all* prescribed components as well as for the random background extracted from initial experimental or theoretical data by use of the Helming method (Helming et al., 1994; Helming, 1996).

After having mapped the initial texture components by decomposing them into a group of single orientations which are arranged in the form of a lateral and spherical distribution on the mesh (Fig. 6), the texture component concept is no longer required in the further procedure. During the subsequent crystal plasticity finite element simulation each individual orientation originally pertaining to one of the texture components can undergo *individual* orientation change as in the conventional crystal plasticity methods. This means that the texture component method loses its significance during the simulation.

In order to avoid confusion one should, therefore, underline that the texture component method is used to *feed* textures into finite element simulations on a strict physical and quantitative basis. The components as such, however, are in their original form as compact functions not tracked during the simulation. On the other hand the mapped orientation points which were extracted from the components must not be confused with individual grains, but they mark points of an exact distribution function.
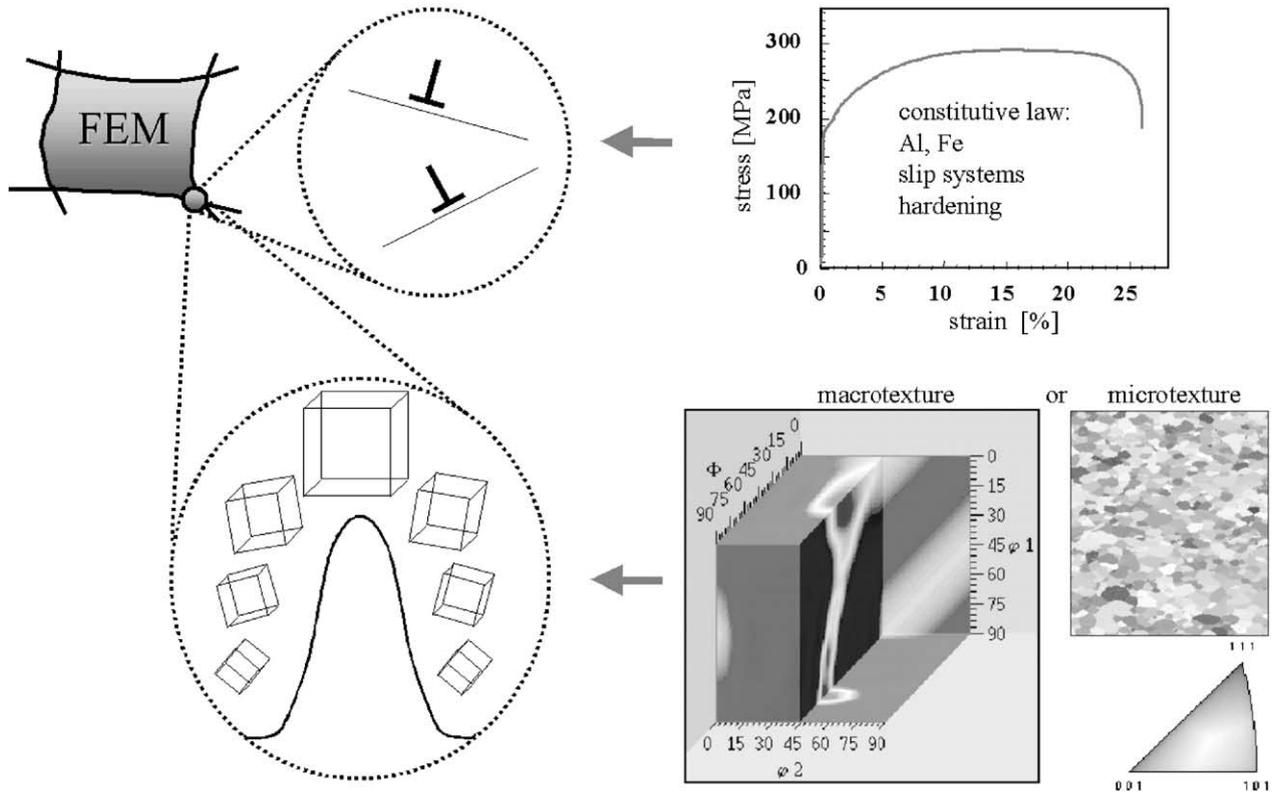
Fig. 3. Principle of the texture component crystal plasticity finite element method (Zhao et al., 2001; Raabe et al., 2001a,b).
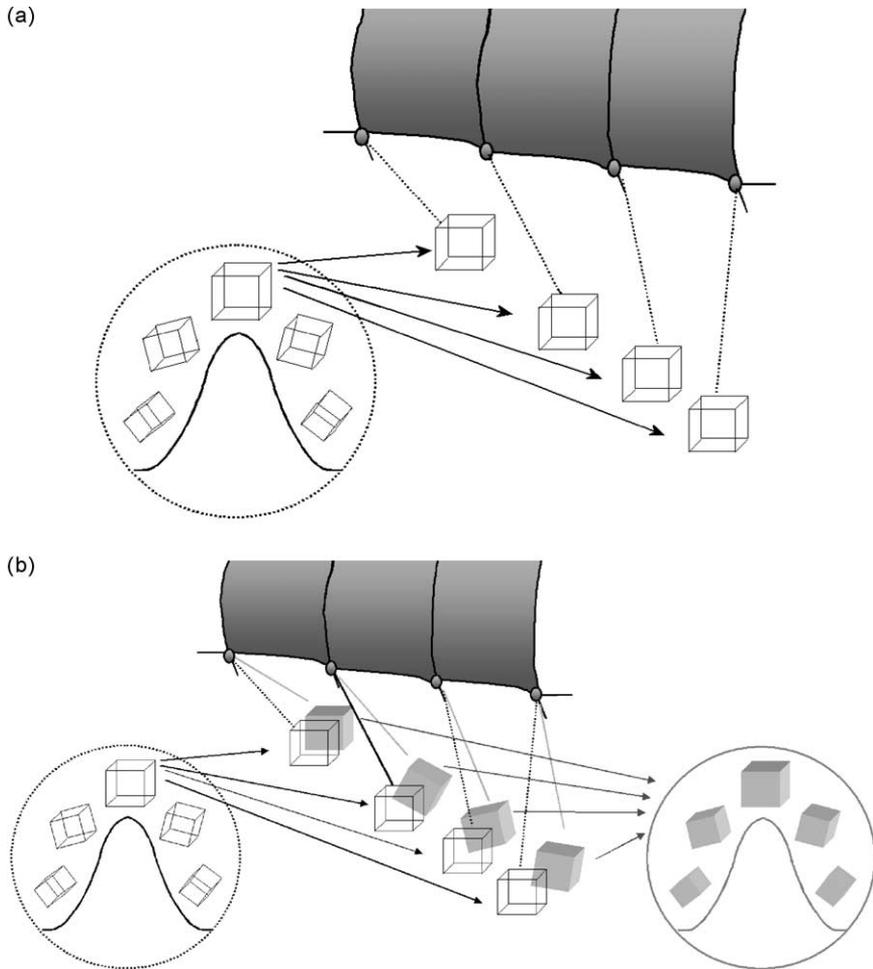
Fig. 4. Schematic drawing showing the first step of the spherical decomposition of a texture component. (a) In the first step the discrete preferred orientation (center or mean orientation of the texture component) is extracted from the texture component and assigned in terms of its respective Euler triple (φ_1, φ, φ_2), i.e. in the form of a single identical rotation matrix, onto each integration point. In this state the sample is a simple single crystal. (b) In the second step, the mapped single orientations taken from the center of the texture component are systematically rotated in such a fashion that their resulting overall distribution reproduces exactly the original texture function which was prescribed in the form of a texture component.

7. Simulation results and experimental results

In the following we present some cup drawing applications of the new texture component crystal plasticity finite element simulation method. Simulations of cup drawing tests, particularly those which aim at predicting the shape change, depend on details of the contact situation between tool and specimen. The present cup
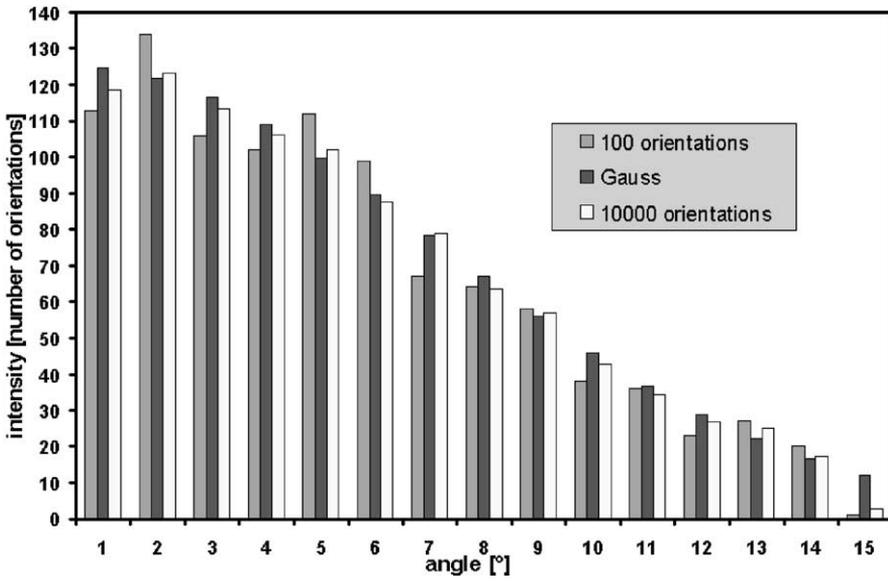
Fig. 5. This diagram shows the agreement between the original Gauss shape of the texture component and the distribution function obtained after decomposing such a function into a set of single orientations.
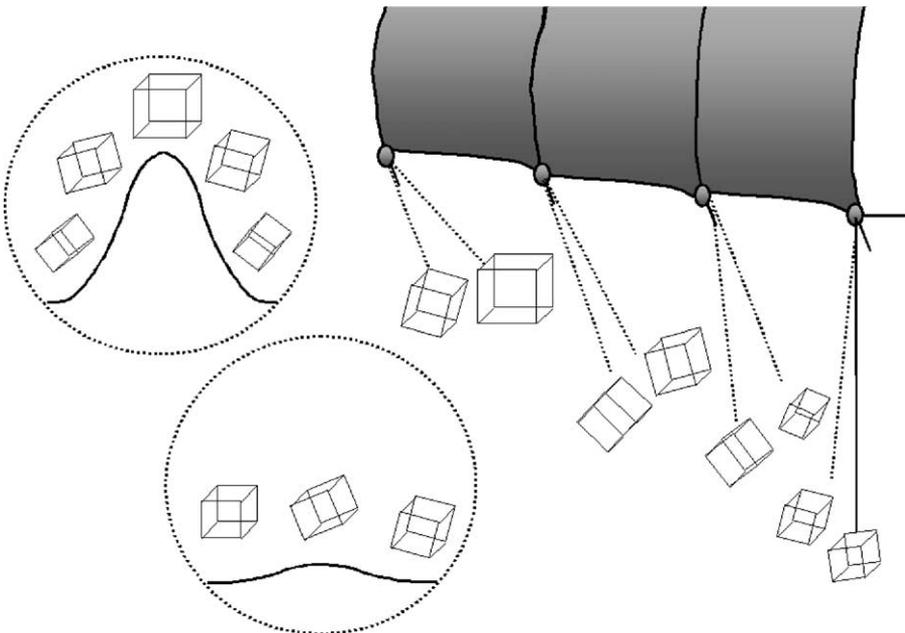

Fig. 6. Schematic drawing showing the mapping of different texture components on a mesh.

drawing simulations were conducted under the assumption that the circular blank being drawn had an initial radius of 100 mm and an initial thickness of 0.82 mm. The blank was modeled using 432 elements of type C3D8 and 80 elements of type C3D6. The interaction between the blank and the blank holder was assumed as a soft contact to impose the appropriate clamping pressure in the thickness direction of the element between blank, die, and blank holder. The simulations used an exponential soft contact function. Different friction properties ($\mu = 0$–0.2) were checked and the results showed that friction properties had under these contact conditions only little influence on the *relative* ear height. This is an important aspect compared to conventional J2-based continuum plasticity simulations which generally reveal stronger dependence on friction. Consequently the $\mu = 0$ case was selected to save computing time. It must be noted though that the influence of friction might be significantly different under different boundary conditions. Since the present simulations were performed without directly feeding the random texture component into the starting configuration, all results were rescaled after the finite element calculation by use of the random volume portion which was suggested by the texture component fit method. All simulations which are presented in the following are compared to experiments (Fig. 7).

Fig. 8 shows the simulated and experimentally observed development of plastic earing in a cup drawn aluminium sample together with the experimental and recalculated {111} pole figures. The texture component fit was performed using only two texture components and a random scattering background component where the latter was used to calibrate the results. The figure compares the texture component finite element simulation with a result obtained by use of a Hill 48 yield surface which was shaped by using experimental *R*-values. The results show that the texture component finite element simulation fits the experimental results somewhat better than that obtained by help of the Hill yield surface. It must be noted in this context that the Hill-based yield surface simulation is not capable of updating anisotropy during loading. The major discrepancy between the Hill-based simulation and the experiment is that the Hill approach does not properly predict the angular position of the maximum relative earing height (Fig. 8). The texture component method yields a better result for the position of the earing maximum and also shows better agreement for the shape of the earing curve particularly for larger angles.

Fig. 9 shows simulation results for a specimen the texture of which was approximated using a volume fraction of 70.97% of an orientation close to the cube component (Euler angles at Gauss maximum: $\varphi_1 = 197.87°$, $\varphi = 6.47°$, $\varphi_2 = 245.00°$) and the rest as random texture background component. The texture recalculated by the component method given in terms of {111} and {200} pole figure projections shows good agreement with the original experimental data. The pole figures are shown in stereographic projections using 1.0, 2.0, 3.0, 4.0, 7.0 contour levels. The predicted distribution of the relative earing height reveals a very good correspondence with the simulation result. Fig. 10 shows a similar example where earing was predicted for an aluminum sample with an initial cold rolling texture. The use of the fitted random background of 32 vol.% does not yield a satisfactory result in the finite element prediction. In order to achieve a good correspondence between simulation and
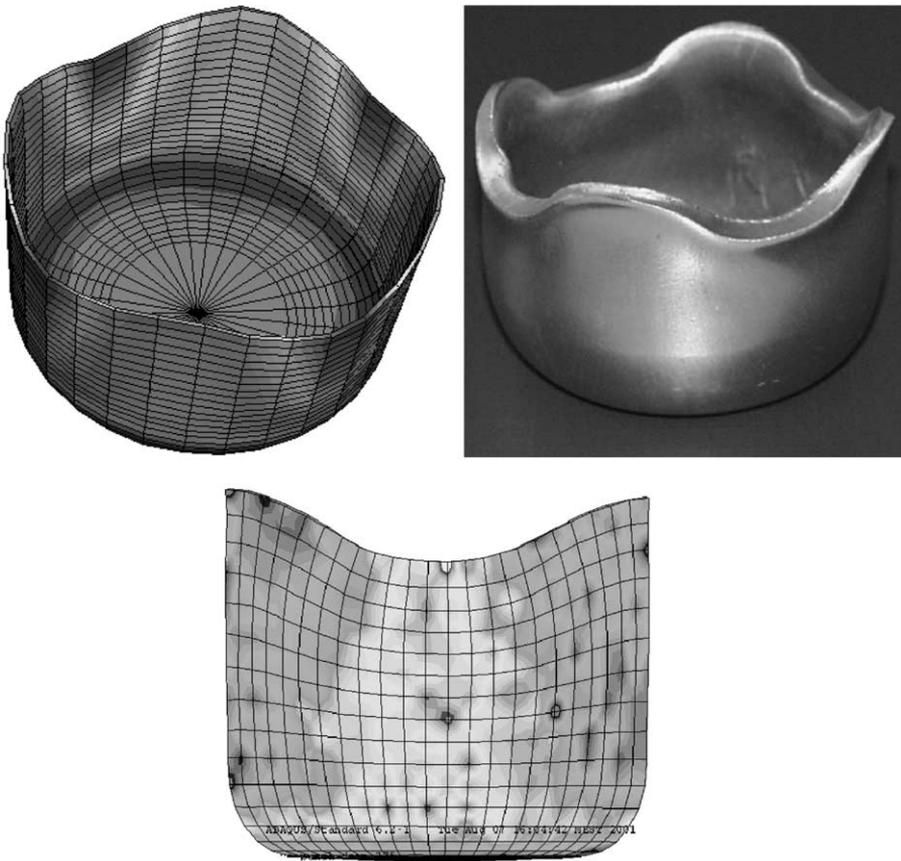
Fig. 7. Left: simulation of a cup drawing test with aluminium. The gray scale indicates the sheet thickness; right: Experimental result; bottom, center: local orientation changes during drawing. The gray scale indicates the orientation change between the initial orientations and the orientations after drawing for one of the used texture components.

experiment a value of 68% random would have to be used. This means that the subsequent calibration of the earing results by use of the initial random texture background component does not give a satisfactory solution. In a subsequent work we will, therefore, present how a random texture component can be directly fed into the finite element approach. From a physical viewpoint the direct incorporation of a random component into the finite element simulation is also pertinent since the crystals represented by such a component can individually evolve into pronounced orientations during the texture simulation. In other words, the random texture component does not remain constant during loading but decreases due to texture formation.
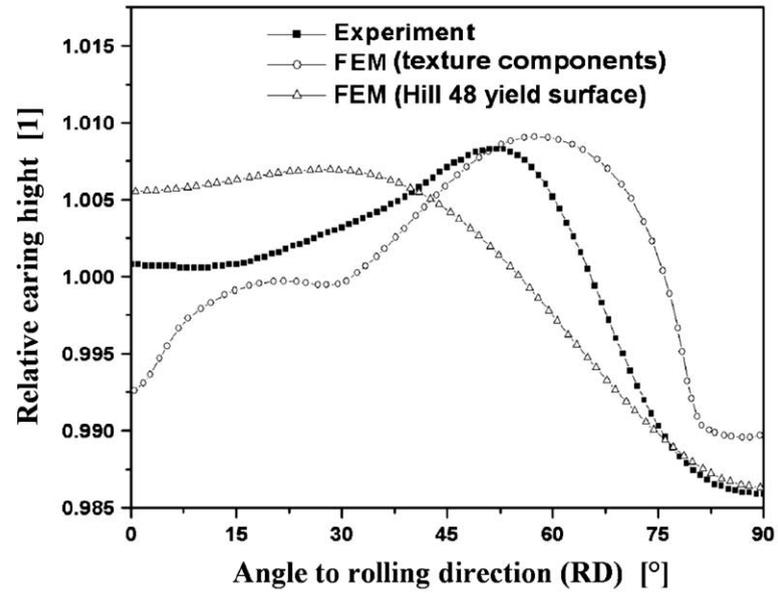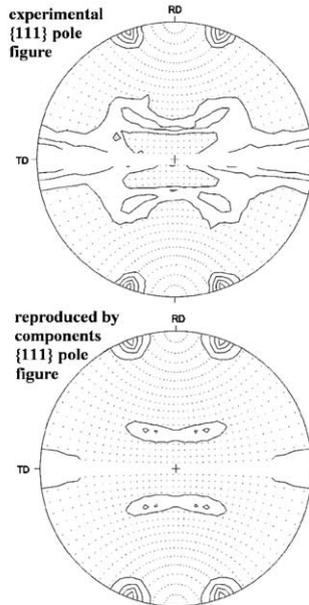
Fig. 8. Left: experimental and reproduced {111} pole figures. Right: simulations and experiment of earing during cup drawing of aluminium. The figure compares the texture component finite element simulation with a simulation obtained by use of a Hill 48 yield surface using experimental *R*-values.
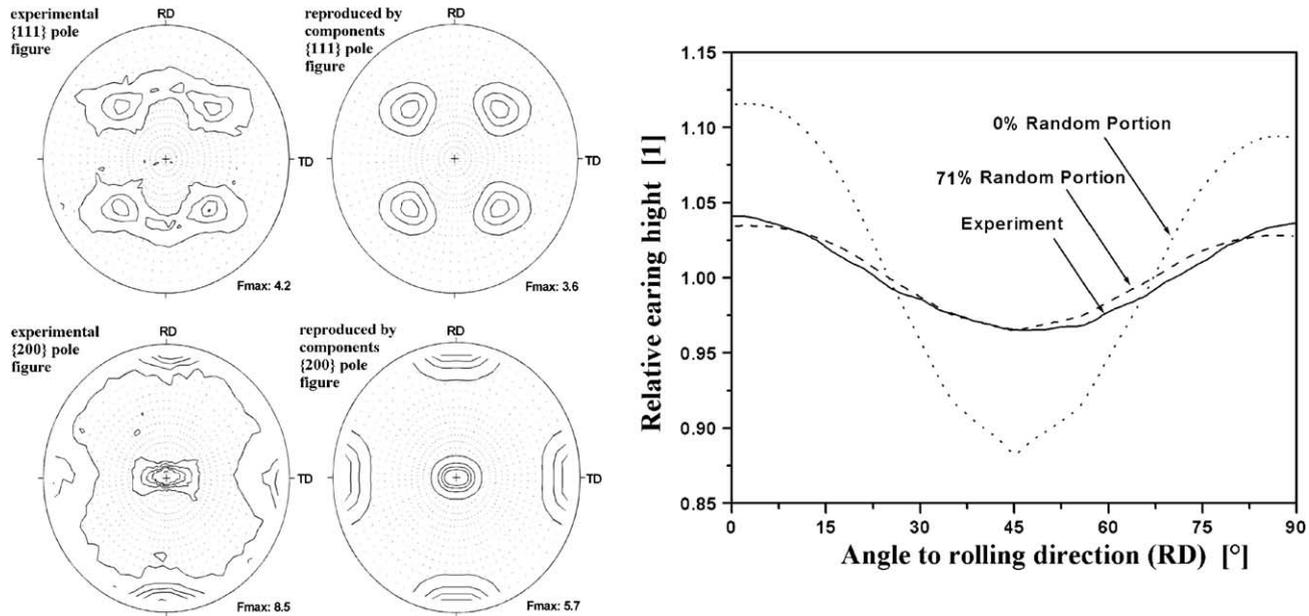
Fig. 9. Simulation and experimental results for earing in an aluminum sample the texture of which was approximated using a volume fraction of 70.97% of an orientation close to the cube component (Euler angles at Gauss maximum: $\varphi_1 = 197.87°$, $\varphi = 6.47°$, $\varphi_2 = 245.00°$) and the rest as random texture background component. The recalculated texture shows good agreement with the original experimental pole figure. The predicted distribution of the relative earing height reveals a very good correspondence with the simulation result.
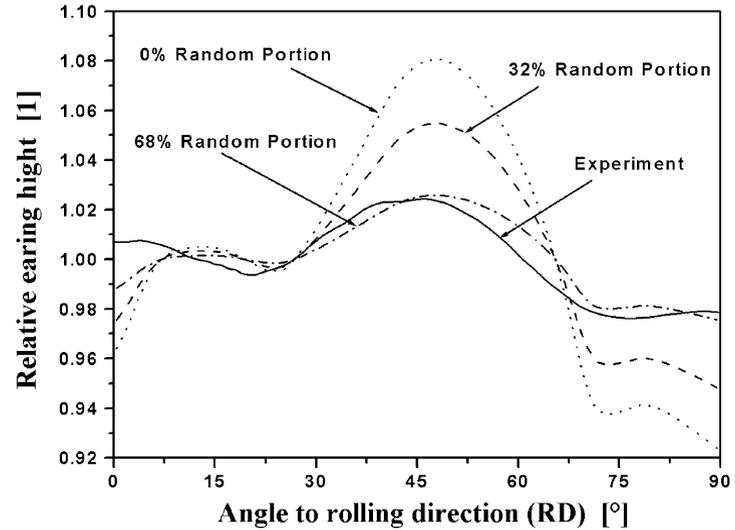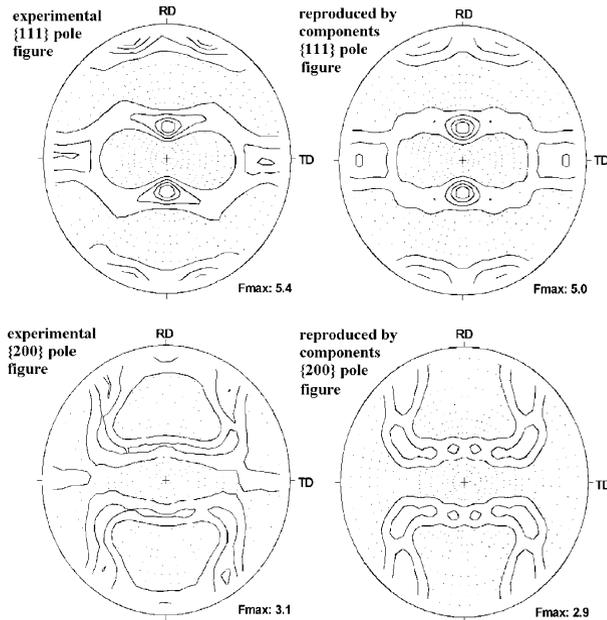
Fig. 10. Simulation and experimental results for earing in an aluminum sample the texture of which was approximated using two rolling texture components and a random texture component. The use of the fitted random background of 32 vol.% does not yield a satisfactory result in the finite element prediction. In order to achieve a good correspondence between simulation and experiment a value of 68% random had to be used.

8. Conclusions

The study presented a new finite element method which includes and updates texture during forming simulations. The method is based on feeding discrete localized spherical texture components onto the Gauss points of the mesh of a finite element simulation which uses a crystal plasticity constitutive law. The method was tested and the results were compared to experimental data and to yield surface simulations.

References

Asaro, R.J., Needleman, A., 1985. Texture development and strain hardening in rate dependent polycrystals. Acta Metall. 33, 923–941.

Beaudoin, A.J., Dawson, P.R., Mathur, K.K., Kocks, U.F., 1995. A hybrid finite-element formulation for polycrystal plasticity with consideration of macrostructural and microstructural linking. Int. J. Plasticity 11, 501–521.

Beaudoin, A.J., Mecking, H., Kocks, U.F., 1996. Development of localized orientation gradients in fcc polycrystals. Philos. Mag. A73, 1503–1518.

Bhattacharyya, A., El-Danaf, E., Kalidindi, S.R., Doherty, R.D., 2001. Evolution of grain-scale microstructure during large strain simple compression of polycrystalline aluminum with quasi-columnar grains: OIM measurements and numerical simulations. Int. J. Plasticity 17, 861–883.

Bunge, H.J., 1982. Texture Analysis in Materials Science. Butterworths, London, UK.

Bunge, H.J., 1987. Theoretical Methods of Texture Analysis. Deutsche Gesellschaft für Materialkunde DGM Informationsgesellschaft, Frankfurt, Germany.

Dahms, M., Beaven, P.A., Tobisch, J., Bermig, G., Helming, K., 1994. Texture analysis of titanium aluminide—comparison of the component and the positivity method. Zeitschr. Metallkunde 85, 536544.

Eschner, Th., 1994. Quantitative Texturanalyse durch Komponentenzerlegung von Beugungspolfiguren. PhD Dissertation Thesis, University of Freiberg.

Eschner, Th., Fundenberger, J.J., 1997. Application of anisotropic texture components. Texture and Microstructures 28, 181195.

Hosford, W.F., 1996. On the basis of yield criteria. Textures and Microstructures 26, 479493.

Helming, K., Eschner, Th., 1990. A new approach to texture analysis of multiphase materials using a texture component model. Cryst. Res. Technol. 25, K203K208.

Helming, K., Schwarzer, R.A., Rauschenbach, B., Geier, S., Leiss, B., Wenk, H.-R., Ullemeier, K., Heinitz, J., 1994. Texture estimates by means of components. Zeitschr. Metallkunde 85, 545553.

Helming, K., 1996. Texturapproximation durch Modellkomponenten (in German). Habilitation Thesis, Technical University Clausthal, Germany, Cuvillier Verlag Göttingen, Germany.

Kalidindi, S.R., Bronkhorst, C.A., Anand, L., 1992. Crystallographic texture evolution during bulk deformation processing of fcc metals. J. Mech. Phys. Solids 40, 537569.

Kalidindi, S.R., 2001. Modeling anisotropic strain hardening and deformation textures in low stacking fault energy fcc metals. Int. J. Plasticity 17, 837–860.

Kocks, U.F., Tomé, C., Wenk, H.-R., 1997. Texture and Anisotropy. Preferred Orientations in Polycrystals and Their Effect on Material Properties. Cambridge University Press, Cambridge, UK.

Kok, S., Beaudoin, A.J., Tortorelli, D.A., 2002. A polycrystal plasticity model based on the mechanical threshold. Int. J. Plasticity 18, 715–741.

Lücke, K., Pospiech, J., Virnich, K.H., Jura, J., 1981. On the problem of the reproduction of the true orientation distribution from pole figures. Acta Metall. 29, 167185.

Lücke, K., Pospiech, J., Jura, J., Hirsch, J., 1986. On the presentation of orientation distribution functions by model functions. Zeitschr. Metallkunde 77, 312321.

Mathur, K.K., Dawson, P.R., 1989. On modeling the development of crystallographic texture in bulk forming processes. Int. J. Plasticity 5, 67–94.

Matthies, S., Wenk, H.-R., Vinel, G.W., 1988. Some basic concepts of texture analysis and comparison of three methods to calculate orientation distributions from pole figures. J. Appl. Cryst. 21, 285304.

Matthies, S., 1982. Form effects in the description of the orientation distribution function of texturized materials by model components. Physica Status Solidi (b) 112, 705716.

Matthies, S., 1991. On the principle of conditional ghost correction and its realization in existing correction concepts. Textures and Microstructures, 14– 18, 1–12.

Matthies, S., Vinel, G. W., Helming, K., 1987–1990. Standard Distributions in Texture Analysis, Vols. I–III. Akademie Verlag, Berlin, Germany.

Mika, D.P., Dawson, P.R., 1999. Polycrystal plasticity modeling of intercrystalline boundary textures. Acta Mater. 47, 13551369.

Nakamachi, E., Xie, C.L., Morimoto, H., Morita, K., Yokoyama, N., 2002. Formability assessment of FCC aluminum alloy sheet by using elastic/crystalline viscoplastic finite element analysis. Int. J. Plasticity 18, 617–632.

Raabe, D., 1995a. Examination of the iterative series-expansion method for quantitative texture analysis. Textures and Microstructures 23, 115129.

Raabe, D., 1995b. Texture simulation for hot rolling of aluminium by use of a Taylor model considering grain interactions. Acta Metall. 43, 10231028.

Raabe, D., Lücke, K., 1993. Investigation of the ADC method for direct ODF approximation by means of standard functions. Physica Status Solidi (b) 180, 5965.

Raabe, D., Lücke, K., 1994. Analysis of the ADC method for direct ODF calculation by use of Gauss models and standard function. Materials Science Forum 157– 162, 413–418.

Raabe, D., Becker, R., 2000. Coupling of a crystal plasticity finite element model with a probabilistic cellular automaton for simulating primary static recrystallization in aluminum. Modeling and Simulation in Materials Science and Engineering 8, 445462.

Raabe, D., Sachtleber, M., Zhao, Z., Roters, F., Zaefferer, S., 2001a. Micromechanical and macromechanical effects in grain scale polycrystal plasticity experimentation and simulation. Acta Mater. 49, 3433–3441.

Raabe, D., Zhao, Z., Roters, F., 2001b. A finite element method on the basis of texture components for fast predictions of anisotropic forming operations. Steel Research 72, 421–426.

Raabe, D., Zhao, Z., Park, S.-J., Roters, F., 2002a. Theory of orientation gradients in plastically strained crystals. Acta Mater. 50, 421–440.

Raabe, D., Roters, F., Zhao, Z., 2002b. A texture component crystal plasticity finite element method for physically-based metal forming simulations including texture update. Materials Science Forum, 396-402, 31–36.

Raabe, D., Zhao, Z., Mao, W., 2002c. On the dependence of in-grain subdivision and deformation texture of aluminium on grain interaction. Acta Mater. 50, 4379–4394.

Sarma, G.B., Dawson, P.R., 1996. Texture predictions using a polycrystal plasticity model incorporating neighbor interactions. Int. J. Plasticity 12, 1023–1054.

Van Houtte, P., Delannay, L., Kalidindi, S.R., 2002. Comparison of two grain interaction models for polycrystal plasticity and deformation texture prediction. Int. J. Plasticity 18, 359–377.

Wassermann, G., Grewen, J., 1969. Texturen metallischer Werkstoffe. Springer-Verlag, Berlin, Germany (in German).

Wenk, H.-R., Bunge, H. J., Kalend, J. S., Lücke, K., Matthies, S., Pospiech, J. and Van Houtte, P., 1988. Orientation distributions: representation and determination. In: Proceedings Eighth International Conference on Textures of Materials (ICOTOM 8). The Metallurgical Society, Warrendale, PA, USA, pp. 17–30.

Zhao, Z., Roters, F., Mao, W., Raabe, D., 2001. Introduction of a texture component crystal plasticity finite element method for industry-scale anisotropy simulations. Adv. Eng. Mat. 3, 984–990.

Zhou, Y., Jonas, J.J., Savoie, J., Makinde, A., MacEwen, S.R., 1998. Effect of texture on earing in FCC metals: finite element simulations. Int. J. Plasticity 14, 117–138.